HHS Public Access

Author manuscript

Virology. Author manuscript; available in PMC 2022 July 08.

Published in final edited form as:

Virology. 2017 June ; 506: 45–54. doi:10.1016/j.virol.2017.03.007.

Isolation and characterization of a novel putative human polyomavirus

Tarik Gheit[a], **Sankhadeep Dutta**[a], **Javier Oliver**[a], **Alexis Robitaille**[a], **Shalaka Hampras**[b], **Jean-Damien Combes**[a], **Sandrine McKay-Chopin**[a], **Florence Le Calvez-Kelm**[a], **Neil Fenske**[c,d], **Basil Cherpelis**[c,d], **Anna R. Giuliano**[e], **Silvia Franceschi**[a], **James McKay**[a], **Dana E. Rollison**[b], **Massimo Tommasino**[a,*]

[a]International Agency for Research on Cancer, World Health Organization, Lyon 69372, France

[b]Department of Cancer Epidemiology, Moffitt Cancer Center, Tampa, FL, USA

[c]Department of Dermatology & Cutaneous Surgery, University of South Florida, Morsani College of Medicine, Tampa, FL, USA

[d]Department of Cutaneous Oncology, Moffitt Cancer Center, Tampa, FL, USA

[e]Center for Infection Research in Cancer, Moffitt Cancer Center, Tampa, FL, USA

Abstract

The small double-stranded DNA polyomaviruses (PyVs) form a family of 73 species, whose natural hosts are primarily mammals and birds. So far, 13 PyVs have been isolated in humans, and some of them have clearly been associated with several diseases, including cancer. In this study, we describe the isolation of a novel PyV in human skin using a sensitive degenerate PCR protocol combined with next-generation sequencing. The new virus, named Lyon IARC PyV (LIPyV), has a circular genome of 5269 nucleotides. Phylogenetic analyses showed that LIPyV is related to the raccoon PyV identified in neuroglial tumours in free-ranging raccoons.

Analysis of human specimens from cancer-free individuals showed that 9 skin swabs (9/445; 2.0%), 3 oral gargles (3/140; 2.1%), and one eyebrow hair sample (1/439; 0.2%) tested positive for LIPyV.

Future biological and epidemiological studies are needed to confirm the human tropism and provide insights into its biological properties.

Keywords

New polyomavirus; Human; Skin

[*]Correspondence to: Infections and Cancer Biology Group, International Agency for Research on Cancer, 150 cours Albert Thomas, 69372 Lyon Cedex 08, France. icb@iarc.fr (M. Tommasino).

1. Introduction

Members of the polyomaviruses (PyVs) are non-enveloped double-stranded DNA viruses with a genome of approximately 5000 nucleotides. The organization of the viral genome is highly conserved throughout the PyV family and comprises early and late coding regions and the viral non-coding control region (NCCR) of approximately 500 bp. The early region encodes for two regulatory proteins: small T-antigen (ST-Ag) and large T antigen (LT-Ag). The late region encodes for three viral proteins that are necessary for formation of the capsid: the major capsid protein VP1 and two minor capsid proteins, VP2 and VP3. The NCCR contains the origin of DNA replication, regulatory elements, and transcription promoters (Moens et al., 2008).

With the development of high-performance molecular biology tools, many of the PyVs have been isolated during the past decade, mainly from mammals, birds, and fish (Johne et al., 2011; Peretti et al., 2015). Based on the observed distance between LT-Ag coding sequences, the International Committee on Taxonomy of Viruses (ICTV) Polyomaviridae Study Group has classified the different species of PyVs into four genera: alpha-, beta-, gamma- and delta-PyV) (Calvignac-Spencer et al., 2016).

To date, a total of 13 PyVs have been isolated from humans: BKPyV (Gardner et al., 1971), JCPyV (Padgett et al., 1971), KIPyV (Allander et al., 2007), WUPyV (Gaynor et al., 2007), Merkel cell PyV (MCPyV) (Feng et al., 2008), human PyV 6 (HPyV6) (Schowalter et al., 2010), human PyV 7 (HPyV7) (Schowalter et al., 2010), trichodysplasia spinulosa-associated PyV (TSPyV) (van der Meijden et al., 2010), human PyV 9 (HPyV9) (Scuda et al., 2011), Malawi PyV (MWPyV) (Siebrasse et al., 2012), Saint Louis PyV (STLPyV) (Lim et al., 2013), human PyV 12 (HPyV12) (Korup et al., 2013) and New Jersey PyV (NJPyV) (Mishra et al., 2014). PyVs are widely spread in the human population. Many PyV infections occur early in life, and in most cases it remains asymptomatic (Nickeleit et al., 2015). Serological studies have shown that up to 90% of the human population has been exposed to HPyV, with several HPyV infections occurring during childhood (Egli et al., 2009; Kean et al., 2009; Sroller et al., 2016).

Four HPyVs have been clearly associated with human diseases, many occurring more frequently in immunocompromised individuals. JCPyV has been associated with progressive multifocal leukoencephalopathy, a fatal brain disease, in immunocompromised individuals (Jiang et al., 2009; Koralnik, 2006), and BKPyV has been associated with nephropathy and hemorrhagic cystitis (Azzi et al., 1994; Coleman et al., 1978), particularly among kidney transplant patients; MCPyV has been isolated from Merkel cell carcinomas of the skin (Feng et al., 2008), a cancer with higher incidence in immunocompromised individuals, and TSVPyV has been associated with a rare cutaneous condition, trichodysplasia spinulosa, in an immunocompromised patient (van der Meijden et al., 2010). A possible association between HPyV7 and non-neoplastic diseases in immunosuppressed individuals has also been reported recently (Ho et al., 2015; Toptan et al., 2016). In addition, HPyV7 has been found in human thymic epithelial tumours, but a causal association has not been established (Rennspiess et al., 2015). The remaining PyVs that have been isolated from humans, KIPyV,

WUPyV, HPyV6, HPyV9, HPyV12, MWPyV, STLPyV and NJPyV, have not so far been associated with any human diseases.

The oncogenic potential of HPyVs has been extensively studied in experimental animal models, where these viruses induce a wide range of tumours. The inoculation of JCPyV in a small rodent model and in non-human primates leads to the development of brain tumours (Miller et al., 1984; Varakis et al., 1978; Walker et al., 1973; Zu Rhein et al., 1979). Transgenic mice expressing the early region of HPyVs have been used to investigate the carcinogenesis induced by MCPyV (Shuda et al., 2015; Verhaegen et al., 2015), JCPyV (Shollar et al., 2004), and BKPyV (Dalrymple et al., 1990). In addition, simian virus 40 (SV40), BKPyV, and JCPyV have been shown to display transforming activity in *in vitro* experimental models (Moens et al., 2008). It is still unclear whether other HPyVs exist. Here, we report the characterization of a new PyV isolated from human skin swabs. We found it to be phylogenetically related to the raccoon PyV (RacPyV) associated with brain tumours in free-ranging raccoons, and gave it the provisional name of Lyon IARC PyV (LIPyV).

2. Materials and methods

2.1. Human specimens

Skin swabs, eyebrow hairs and oral gargles from three different ongoing studies aiming to determine the prevalence of human papillomaviruses (HPVs) and HPyVs were used in the present analysis (Franceschi et al., 2015; Hampras et al., 2015, 2014; Nunes et al., 2016; Pierce Campbell et al., 2016, 2013). Skin swabs and eyebrow hairs were collected at baseline from 448 subjects participating in the VIRUSCAN study, an ongoing five-year (2014–2019) prospective cohort study being conducted at Moffitt Cancer Center and the University of South Florida (R01CA177586-01; “Prospective study of cutaneous viral infections and non-melanoma skin cancer”). In addition, 25 cutaneous skin swabs were randomly selected from the HPV Infection in Men (HIM) study, a large, multi-national prospective cohort study of the natural history of HPV infection in men. The 25 skin swabs were collected from men in Tampa, Florida, USA. The HIM study methods have been described in detail previously and are similar to those used in the VIRUSCAN Study (Giuliano et al., 2011). An area of approximately 5×5 cm of the top of the sun-exposed forearm was sprayed with 0.9% saline solution. A cotton-tipped Dacron swab (Digene, Gaithersburg, MD, USA) was then rubbed back and forth a few times to collect exfoliated skin cells. Individual swabs were placed in a separate vial and preserved in Digene Standard Transport Medium (STM). Three or four eyebrow hairs were plucked from each eyebrow using disposable tweezers. The eyebrow hairs with attached follicles were snap-frozen in liquid nitrogen and stored at −80 °C until further use.

We used 140 oral gargles that were collected for the Study of Natural History of HPV Infection and Precancerous Lesions in the Tonsils (SPLIT), which is an ongoing study on the detection of HPV infection and precancerous lesions in age-stratified immunocompetent individuals who underwent tonsillectomy for benign diseases in selected university hospitals across France (Combes et al., In press; Franceschi et al., 2015).

After DNA extraction, all samples were analysed at the International Agency for Research on Cancer (Lyon, France) for HPVs and all known HPyVs.

2.2. Design of degenerate primers and PCR conditions for PyV screening

Complete HPyV sequences were obtained from GenBank and were used for alignment of the early region genes. A pair of degenerate primers was developed based on the more conserved parts of LT-Ag of several PyV genomes. The accession numbers of the GenBank sequences that were used as references, with the corresponding HPyV types given in parentheses, are EU37584 (MCPyV), NC_001538 (BKPyV), NC_001669 (SV40), EF520287 (KIPyV), NC_009539 (WUPyV), and NC_001699 (JCPyV). Two oligonucleotides (forward primer, 5′-CAW GCT GTR TIT AGT AAT A-3′ and reverse primer, 5′-RWT TAT TMA CHC CIT TAC-3′), allowing the amplification of a region of approximately 240 bp, were synthesized by MWG Biotech (Ebersberg, Germany). The polymerase chain reaction (PCR) mix contained 1x PCR buffer, 200 μmol/L of each dNTP, 0.2 μmol/L of each primer, and 0.625 U of HotStarTaq DNA polymerase in a final volume of 25 μL (Qiagen). Forty-five amplification cycles were run in the GeneAmp PCR System 2400 with a 94 °C denaturation step (1 min), a 48 °C annealing step (1 min), and a 72 °C extension step (1 min), including an initial denaturation step of 15 min and a final extension step of 10 min, resulting in a 240-bp product.

2.3. Next-generation sequencing

The libraries were prepared using 50 ng of the PCR products with DNA NEBNext Fast DNA Library Prep Set for Ion Torrent (New England Biolabs, Ipswich, MA, USA) following the manufacturer's protocol, and sequenced with the Ion Torrent PGM sequencer (Life Technologies) at 100x coverage using the Ion OneTouch 200 Template Kit v2 DL and the Ion PGM Sequencing 200 Kit v2 with the 314 or 316 chip kits (all produced by Life Technologies), following the manufacturer's instructions. The data analysis was conducted using Geneious version 6.0.1 (http://www.geneious.com) (Kearse et al., 2012).

2.4. Luminex assay for high throughput screening of LIPyV

As described previously, LIPyV DNA from eyebrow hairs, and skin swabs was detected using a highly sensitive and specific assay which combines multiplex PCR and bead-based Luminex technology (Schmitt et al., 2006, 2010). The following PCR primers and Luminex probe were used: forward primer, 5′-CAA GCC TTG CTG CAG CAT TCC TAG-3′ and reverse primer, 5′-ATC TTT GTT TTG TCC TCT AGA ACC CT-3′; and probe, 5′-ATC TAT CTT GGG GGC AAT-3′. Briefly, PCR products were denatured and hybridized to the beads coupled with specific probes for LIPyV. Results were expressed as the median fluorescence intensity (MFI) of at least 100 beads per bead set. For each probe, MFI values with no respective PCR product added to the hybridization mixture were considered background values. The cut-off was computed by adding 5 MFI to 1.1x the median background value.

2.5. Rolling circle amplification

DNA was extracted and purified from skin swabs as described previously (Schowalter et al., 2010). The DNA was amplified by multiply primed rolling circle amplification (RCA) using the Illustra TempliPhi 100 Amplification Kit according to the manufacturer's recommendations (GE Healthcare, Piscataway, NJ), with supplementation of 450 μM dNTPs as described by Rector et al. (2004).

2.6. Long-range PCR

Long-range PCR was performed for amplification of the entire genome using the Takara LA Taq HS polymerase, following the manufacturer's instructions (Takara Bio Inc.). The following primers were used at a final concentration of 0.5 μM each: forward primer, 5′-TAA ATT TTG AGT TGG GTT GTG CAC AAG AT-3′ and reverse primer, 5′-ATC TAT CTT GGG GGC AAT TAA TAT TTA ATG-3′.

2.7. Proofreading PCR

PCR using the proofreading Pfu ultra hot start DNA polymerase (Agilent Technologies, Santa Clara, CA, USA) was performed according to the manufacturer's instructions.

2.8. Cell culture and transient transfection

First, HEK293 cells were cultured in Dulbecco's modified Eagle's medium (DMEM) supplemented with 10% fetal bovine serum (FBS), 100U/ML penicillin G, 100 μg/ML streptomycin, 2 mM L-glutamine (Invitrogen Life Technologies), and 1 mM sodium pyruvate (Sigma-Aldrich). Then, 1.5×10^{5} cells were transiently transfected with 1.0 μg of pcDNA3 expression vector (Invitrogen) containing the early region of LIPyV by using the X-tremeGENE 9 reagent (Roche) according to the manufacturer's protocols. At 48 h after transfection, cells were collected for isolation of total RNA.

2.9. Reverse transcription and qPCR

Total RNA was extracted using the NucleoSpin RNA kit (Macherey-Nagel). The obtained RNA was reverse-transcribed to cDNA with the RevertAid H Minus M-MuLV Reverse Transcriptase kit (ThermoFisher Scientific) according to the manufacturer's instructions. The LIPyV cDNA was amplified by PCR using the following pair of specific primers: forward primer, 5′-AGA ATA TGG TAA TAT ACC ATT AAT GAA GAA TG-3′ and reverse primer 5′-GTG ATC AGA TTG TGA TTT TGC TGA G-3′. The amplicon was purified using the QIAquick gel extraction kit (Qiagen) and sequenced by GATC (GATC Biotech, Germany).

2.10. Phylogenetic analyses

Phylogenetic trees were constructed from the alignments of the nucleotide sequences of LT-Ag and VP1, and the amino acid sequences of LT-Ag from the following 47 avian and mammalian PyVs: budgerigar PyV (NC_004764), crow PyV (NC_007922), finch PyV (NC_007923), goose hemorrhagic PyV (NC_004800), TSPyV (NC_014361), Bornean orangutan PyV1 (NC_013439), chimpanzee PyV (NC_014743), murine PyV (NC_001515), hamster PyV (NC_001663), HPyV9 (NC_015150), African green monkey

PyV (NC_004763), SV40 (NC_001669), BKPyV (NC_001538), JCPyV (NC_001699), simian virus 12 (NC_007611), California sea lion PyV1 (NC_013796), bovine PyV (NC_001442), murine pneumotropic virus (NC_001505), squirrel monkey PyV (NC_009951), HPyV6 (NC_014406), HPyV7 (NC_014407), KIPyV (NC_009238), WUPyV (NC_009539), MWPyV_MA095 (JQ898291), MWPyV_WD976 (JQ898292), STLPyV_MA138 (NC_020106), STL PyV_WD972 (JX463184), raccoon PyV_R45 (JQ178241), raccoon PyV_Rac17 (KU533635), equine PyV (NC_017982), *Artibeus planirostris* PyV3_A504 (JQ958890), *Myotis* PyV (NC_011310), *Mastomys* PyV (AB588640), dolphin PyV1 (KC594077), vervet monkey PyV1 (NC_019844), *Otomops* PyV2 (NC_020066), *Chaerephon* PyV1 (NC_020065), bat PyV_B0454 (JQ958888), *Eidolon* PyV1 (NC_020068), *Pan troglodytes verus* PyV1a (HQ385746), *Pan troglodytes verus* PyV2a (HQ385748), MCPyV (NC_010277), gorilla PyV1 (HQ385752), *Cardioderma* PyV1 (NC_020067), *Otomops* PyV1 (NC_020071), bat PyV (JQ958889) and LIPyV (KY404016).

The sequences were aligned using the MUSCLE algorithm with default parameters (Edgar, 2004a), implemented in MEGA7 (Kumar et al., 2016). MEGA7 was used to test substitution models, and for all the following phylogenetic analysis. Based on the alignment with MUSCLE, all positions with less than 95% site coverage were eliminated (partial deletion), to allow the inclusion of taxa with some missing data. Codon positions included were 1st+2nd+3rd+ non-coding. There were a total of 1011 positions in the final dataset for VP1 nucleotide sequences, 1674 for LT-Ag nucleotide sequences, and 554 for LT-Ag amino acid sequences. A discrete gamma distribution was used to model evolutionary rate differences among sites (five categories; +G, parameter=0.8203 and 1.1058, respectively, for VP1 and LT-Ag nucleotides sequences, and 1.1420 for LT-Ag amino acid sequences). The rate variation model allowed for some sites to be evolutionarily invariable ([+I], 8.6157% sites and 10.0832% sites, respectively, for VP1 and LT-Ag nucleotides sequences, and 8.9514% for LT-Ag amino acid sequences).

The initial trees for the heuristic search were obtained automatically by applying the Neighbour-Joining (NJ)/BioNJ algorithm to the three different matrixes of pairwise distances estimated using the maximum composite likelihood (MCL) approach for the VP1 and LT-Ag nucleotide sequences, and estimated using a Jones–Thornton–Taylor (JTT) model for the LT-Ag amino acid sequences. The initial trees were obtained using the NJ/BioNJ algorithm to have a first representation of the relationships between the sequences according to their genetic distance, because this algorithm produces a single tree.

In the next step, the statistical method used was the maximum likelihood (ML) algorithm, applied with the goal of comparing the initial trees with other trees generated by the ML search, using the likelihood criterion. During this ML run, the parameter values were optimized to converge to the true parameter value, aiming to find the smallest possible variance among all estimates with the same expected value.

For the nucleotide sequences of both VP1 and LT-Ag, the evolutionary history was inferred by using the ML method based on the general time-reversible model (a nucleotide substitution model), whereas for the amino acid sequences of LT-Ag, the evolutionary

history was inferred by using the ML method based on the Le_Gascuel_2008 model (Le and Gascuel, 2008) (an amino acid substitution model).

For all trees, the topology was then optimized using the nearest-neighbour-interchange heuristic (NNI) to improve the likelihood. This heuristic specifies a neighbour relation between two unrooted trees and then swaps their subtrees in an attempt to obtain a tree that has a higher likelihood.

The final trees that are kept are the trees with the highest log likelihood. Five-hundred ML bootstrap replicates were performed and the support for each node annotated onto the ML tree for each of the phylogenetic trees.

2.11. Nucleotide sequence accession number

The sequence of LIPyV was submitted to Gen Bank and was assigned accession number KY404016.

3. Results

3.1. Viral discovery and sequencing of a new polyomavirus

To identify new human PyVs, 25 skin swabs from the HIM study were tested for PyV using a sensitive degenerate PCR that amplifies a region of approximately 240 bp in LT-Ag. Electrophoretic analysis of the PCR products revealed the presence of amplicons of the expected size in 6 skin swab samples (6/25; 24%). The purified PCR products were pooled and sequenced using Ion Torrent technology (Life Sciences). Approximately 1900 reads were obtained, generating 37 contigs. Nucleotide sequence analysis (BLASTn) revealed that a group of 105 reads of approximately 200 bp shared the highest nucleotide sequence similarity (76%) to RacPyV strains (accession numbers KU533635 and JQ178241), thus representing a potential new PyV. The re-analysis by PCR of the 25 skin swabs using specific primers showed that only one skin swab (1/25; 4%) tested positive for the new PyV sequence.

Multiply primed RCA (Johne et al., 2009) was performed on the DNA extracted from the skin swab of a woman aged 65 years, who had previously tested positive for the new PyV sequence by PCR. To obtain the complete viral genome, first, long-range PCR was performed using outward-directed primers specific for the putative new PyV and the RCA product as template, generating an amplicon of approximately 5 kb. Then, by a primer-walking strategy (GATC Biotech, Germany), a sequence of 5269 bp representing a whole circular genome of the PyV was obtained. The sequence was validated twice using a proofreading polymerase followed by Sanger sequencing.

BLASTn analysis of the whole viral genome confirmed the RacPyV as the closest relative among all known PyVs. Moreover, using MUSCLE (Edgar, 2004b), the new PyV showed the highest nucleotide sequence identity (~65%) to RacPyV strains (accession numbers KU533635 and JQ178241). Because PyV sequences that share less than 81% whole-genome nucleotide sequence identity to members of known species are traditionally considered to be

distinct viral species (Buck et al., 2016; Johne et al., 2011), this new species of PyV was given the provisional name of Lyon IARC PyV (LIPyV).

3.2. Genome characterization

The genome of LIPyV is circular and 5269 bp in length (accession number KY404016), encoding open reading frames (ORFs) for all of the major PyV proteins. Analysis of the complete nucleotide sequence showed that the LIPyV genome shares the features of other known PyVs with an early region consisting of ST-Ag and LT-Ag and a late region coding for the VP1, VP2, and VP3 structural proteins. A NCCR (nucleotide positions 1–401) sharing the characteristics of the ori regions of most of the mammalian polyomaviruses was found (Fig. 1A). This region contains six LT-Ag binding sites (An et al., 2012; Pipas, 1992): four GAGGC, one reverse complement GCCTC, and the sixth with the sequence 5′-GTGGC-3′.

The early gene expression region (nucleotide positions 2455–5269) has a length of 2815 bp and contains ORFs encoding for ST-Ag and LT-Ag. To accurately determine the splice donor and splice acceptor giving rise to LT-Ag (Fig. 1B), the entire early region was cloned into an expression vector (pcDNA3), and 293 cells were transfected for 48 h. Reverse transcription PCR (RT-PCR) was performed using the primers spanning a region of 900 bp that most likely harbours the splice sites. An amplicon of 488 bp was obtained and sequenced in order to identify the splice junction, resulting in the identification of a LT ORF of 2403 bp that encodes for a LT-Ag of 800 amino acids. In addition, the RT-PCR experiment enabled the identification of two additional mRNA transcripts that correspond to (i) a splicing of 98 bp within the transcript that gives rise to ST-Ag of 179 amino acids (Shuda et al., 2009), and (ii) a splicing of 222 bp that yields an ORF of 148 amino acids, with the first 138 amino acids shared with ST-Ag. We named this putative protein 148T-Ag (Figs. 1B and 2). Experiments with the entire viral genome may reveal additional alternative mRNA splice variants; however, we do not yet have indications about whether LIPyV could efficiently replicate in *in vitro* experimental models.

As for MCPyV (Carter et al., 2013) or TSPyV (van der Meijden et al., 2015), we identified a putative alternate T antigen ORF (ALTO) overprinted in the +1 frame of the second exon of LIPyV LT (nucleotide positions 4035–4619). This ORF encodes for 194 amino acids (Fig. 1A).

The structure of ST-Ag, LT-Ag and 148T-Ag is shown in Fig. 2 and Table 1. The late region of LIPyV includes ORFs that encode for the VP1 (nucleotide positions 1120–2427), VP2 (nucleotide positions 402–1145), and VP3 (nucleotide positions 630–1145) capsid proteins. The start codon for the VP3 ORF is located within the VP2 ORF, and the start codon for the VP1 ORF overlaps the C-terminal region of the VP2 ORF (Fig. 1A).

3.3. Phylogenetic relationship among polyomaviruses

To investigate the evolutionary history of LIPyV, we constructed ML phylogenetic trees using MEGA7 (Kumar et al., 2016) based on an alignment of the nucleotide sequences of VP1 and LT-Ag (Fig. 3A and B), and on the alignment of the amino acid sequences of LT-Ag (Fig. 3C) of 47 mammalian or avian PyVs. The phylogenies of VP1 and LT-Ag

showed that LIPyV is closely related to RacPyVs. In all trees, LIPyV and RacPyVs clustered significantly with different mammalian PyVs that include one HPyV (MCPyV) and several PyVs isolated from bats (*Otomops, Cardioderma, Eidolon*) or primates (gorilla, *Pan troglodytes verus*, vervet monkey).

3.4. LIPyV prevalence in human specimens

The prevalence of LIPyV in humans was evaluated using a highly specific and sensitive Luminex-based assay (Schmitt et al., 2006, 2010). The analysis was performed on skin swabs and eyebrow hairs collected in the USA from 448 skin cancer screening patients participating in the VIRUSCAN study prospective cohort. The mean age at study enrolment was 69.4 years. The study population included 54.7% women, 96.4% Whites, and 93.4% non-Hispanics. Skin swabs and eyebrow hair samples were obtained at baseline from 445 and 439 individuals, respectively. Based on the Luminex analysis, 9 skin swabs (9/445; 2.0%) and 1 eyebrow hair sample (1/439; 0.2%) tested positive for LIPyV. The LIPyV-positive eyebrow hair sample was obtained from a Hispanic White man aged 79 years. The LIPyV-positive skin swabs were obtained from 4 non-Hispanic White men, 1 Hispanic White man, and 4 non-Hispanic White women, aged 62–81 years. Interestingly, the eyebrow hair follicles and the skin swab collected from one individual both tested positive for LIPyV.

In addition, 140 oral gargles from the SPLIT study were collected in France from 59 women and 81 men, aged 18–67 (mean age=29.3 years). A total of 3 oral gargles (3/140; 2.1%) tested positive for LIPyV. Two women (aged 34 and 51 years) and one man (aged 26 years) were positive for LIPyV.

4. Discussion

Polyomaviridae is a growing family that infects fish, birds, rodents, humans, and non-human primates (Johne et al., 2011; Peretti et al., 2015). With the advent of new molecular tools, the discovery of new PyVs has accelerated over the past decade. However, although a large number of PyVs have been detected in different animals, the discovery of new HPyVs has been less frequent. The latest HPyV (NJPyV) was discovered in 2014 (Mishra et al., 2014). Although most of the HPyV infections are asymptomatic, a few HPyVs may induce diseases or cancer, notably in immunocompromised individuals (Feng et al., 2008; Jiang et al., 2009; van der Meijden et al., 2010).

In the present study, the use of degenerate PCR primers combined with high-throughput sequencing enabled the discovery of a new PyV in human skin specimens. The analysis of the LIPyV genome showed that its organization shares most of the features of other known PyVs, and contains conserved domains that play roles in PyV-induced cell transformation. The N-terminal region of LIPyV LT-Ag contains a LXCXE motif that has the ability to bind pRB family members (Chestukhin et al., 2002; Moens et al., 2007). The pRB binding motif is always preserved after the integration of MCPyV LT into the host genome; in addition, it has been shown to be required in promoting growth of Merkel cell carcinoma cells (Houben et al., 2012; Shuda et al., 2008). LIPyV LT-Ag also has an ATPase domain that contains two highly conserved motifs, GPXXXGKT and GXXXVNLE, that are necessary for complex formation with p53 (Pipas, 1992). LIPyV ST-Ag contains two PP2A binding sites. Several

ST-Ag PyVs (BKPyV, JCPyV, MuPyV, SV40, and MCPyV) have the ability to interact and inhibit PP2A phosphatase activity. SV40 ST-Ag alters PP2A activity by interacting with the PP2A scaffolding A subunit; the loss of this interaction impairs the tumorigenic activity of ST-Ag (Cho et al., 2007; Guergnon et al., 2011; Kwun et al., 2015; Sablina et al., 2008; Yu et al., 2001). However, *in vitro* experimental studies are required to demonstrate the ability of LIPyV to replicate in human cells, and to characterize the biological activity of its viral proteins; such studies will make it possible to predict the potential role of this newly discovered PyV in human transformation.

LIPyV shares approximately 65% sequence identity with RacPyV, a PyV that has been found in brain tumours from raccoons (Dela Cruz et al., 2013). This proximity with the RacPyV strains has been confirmed by a phylogenetic analysis based on the LT-Ag and VP1 ORFs and suggests an oncogenic potential of LIPyV. In the present study, human specimens collected from different anatomical sites in individuals from subjects in the USA and France were tested for LIPyV, showing a relatively low prevalence of approximately 2% in oral gargles and skin swabs. Interestingly, the eyebrow hair follicles and the skin swab collected from one individual were both positive for LIPyV, which may suggest a possible replication and shedding of this virus in the human host. Moreover, this prevalence is comparable to those observed for other human PyVs in stool, blood, cerebrospinal fluid, urine, or respiratory specimens (Li et al., 2015; Lim et al., 2013; Rockett et al., 2013; Siebrasse et al., 2012).

It is also possible that LIPyV has a tropism for other anatomical sites that still need to be elucidated. In addition, we cannot exclude the possibility that LIPyV is an animal virus and its presence in the human body may represent an environmental contamination. However, the detection of LIPyV DNA in eyebrow hair follicles does not support this hypothesis. Serological studies aiming to determine the presence of antibodies against LIPyV in human sera will further clarify this issue and will conclusively demonstrate whether LIPyV represents the 14th HPyV.

Acknowledgments

We are grateful to Mrs Nicole Suty for her help with manuscript preparation and Dr Karen Müller for editing. This study was supported in part by the European Commission, Grant HPV-AHEAD (FP7-HEALTH-2011-282562), by the Grant VIRUSCAN R01 (No. R01CA177586-01), and by a grant from Fondation ARC (No. PJA 20151203192).

References

Allander T, Andreasson K, Gupta S, Bjerkner A, Bogdanovic G, Persson MA, Dalianis T, Ramqvist T, Andersson B, 2007. Identification of a third human polyomavirus. J. Virol 81, 4130–4136. [PubMed: 17287263]

An P, Saenz Robles MT, Pipas JM, 2012. Large T antigens of polyomaviruses: amazing molecular machines. Annu. Rev. Microbiol 66, 213–236. [PubMed: 22994493]

Azzi A, Fanci R, Bosi A, Ciappi S, Zakrzewska K, de Santis R, Laszlo D, Guidi S, Saccardi R, Vannucchi AM, et al. , 1994. Monitoring of polyomavirus BK viruria in bone marrow transplantation patients by DNA hybridization assay and by polymerase chain reaction: an approach to assess the relationship between BK viruria and hemorrhagic cystitis. Bone Marrow Transplant. 14, 235–240. [PubMed: 7994238]

Buck CB, Van Doorslaer K, Peretti A, Geoghegan EM, Tisza MJ, An P, Katz JP, Pipas JM, McBride AA, Camus AC, McDermott AJ, Dill JA, Delwart E, Ng TF, Farkas K, Austin C, Kraberger S, Davison W, Pastrana DV, Varsani A, 2016. The ancient evolutionary history of polyomaviruses. PLoS Pathog. 12, e1005574. [PubMed: 27093155]

Calvignac-Spencer S, Feltkamp MC, Daugherty MD, Moens U, Ramqvist T, Johne R, Ehlers B, 2016. A taxonomy update for the family Polyomaviridae. Arch. Virol 161, 1739–1750. [PubMed: 26923930]

Carter JJ, Daugherty MD, Qi X, Bheda-Malge A, Wipf GC, Robinson K, Roman A, Malik HS, Galloway DA, 2013. Identification of an overprinting gene in Merkel cell polyomavirus provides evolutionary insight into the birth of viral genes. In: Proceedings of the National Academy of Sciences of the United States of America, vol. 110. pp. 12744–12749. [PubMed: 23847207]

Chestukhin A, Litovchick L, Rudich K, DeCaprio JA, 2002. Nucleocytoplasmic shuttling of p130/RBL2: novel regulatory mechanism. Mol. Cell. Biol 22, 453–468. [PubMed: 11756542]

Cho US, Morrone S, Sablina AA, Arroyo JD, Hahn WC, Xu W, 2007. Structural basis of PP2A inhibition by small t antigen. PLoS Biol. 5, e202. [PubMed: 17608567]

Coleman DV, Mackenzie EF, Gardner SD, Poulding JM, Amer B, Russell WJ, 1978. Human polyomavirus (BK) infection and ureteric stenosis in renal allograft recipients. J. Clin. Pathol 31, 338–347. [PubMed: 205555]

Combes JD, Dalstein V, Gheit T, Clifford GM, Tommasino M, Clavel C, Lacau St Guily J, Franceschi S, SPLIT study group. 2017. Prevalence of human papillomavirus in tonsil brushings and gargles in cancer-free patients: The SPLIT studyOral. Oncol. 66, 52–57.

Dalrymple SA, Beemon KL, 1990. BK virus T antigens induce kidney carcinomas and thymoproliferative disorders in transgenic mice. J. Virol 64, 1182–1191. [PubMed: 2154603]

DeCaprio JA, Garcea RL, 2013. A cornucopia of human polyomaviruses. Nature reviews. Microbiology 11, 264–276. [PubMed: 23474680]

DeCaprio JA, Ludlow JW, Figge J, Shew JY, Huang CM, Lee WH, Marsilio E, Paucha E, Livingston DM, 1988. SV40 large tumor antigen forms a specific complex with the product of the retinoblastoma susceptibility gene. Cell 54, 275–283. [PubMed: 2839300]

Dela Cruz FN Jr., Giannitti F, Li L, Woods LW, Del Valle L, Delwart E, Pesavento PA, 2013. Novel polyomavirus associated with brain tumors in free-ranging raccoons, western United States. Emerg. Infect. Dis 19, 77–84. [PubMed: 23260029]

Edgar RC, 2004a. MUSCLE: a multiple sequence alignment method with reduced time and space complexity. BMC Bioinform. 5, 113.

Edgar RC, 2004b. MUSCLE: multiple sequence alignment with high accuracy and high throughput. Nucleic Acids Res. 32, 1792–1797. [PubMed: 15034147]

Egli A, Infanti L, Dumoulin A, Buser A, Samaridis J, Stebler C, Gosert R, Hirsch HH, 2009. Prevalence of polyomavirus BK and JC infection and replication in 400 healthy blood donors. J. Infect. Dis 199, 837–846. [PubMed: 19434930]

Ehlers B, Moens U, 2014. Genome analysis of non-human primate polyomaviruses. Infect. Genet. Evol.: J. Mol. Epidemiol. Evolut. Genet. Infect. Dis 26, 283–294.

Feng H, Shuda M, Chang Y, Moore PS, 2008. Clonal Integration of a Polyomavirus in Human Merkel Cell Carcinoma 319. Science, New York, N.Y, 1096–1100.

Franceschi S, Combes JD, Dalstein V, Caudroy S, Clifford G, Gheit T, Tommasino M, Clavel C, Lacau St Guily J, Birembaut P, 2015. Deep brush-based cytology in tonsils resected for benign diseases. Int. J. Cancer 137, 2994–2999. [PubMed: 26111735]

Gardner SD, Field AM, Coleman DV, Hulme B, 1971. New Human Papovavirus (B.K.) Isolated from Urine after Renal Transplantation 1. Lancet, London, England, 1253–1257.

Gaynor AM, Nissen MD, Whiley DM, Mackay IM, Lambert SB, Wu G, Brennan DC, Storch GA, Sloots TP, Wang D, 2007. Identification of a novel polyomavirus from patients with acute respiratory tract infections. PLoS Pathog. 3, e64. [PubMed: 17480120]

Giuliano AR, Lee JH, Fulp W, Villa LL, Lazcano E, Papenfuss MR, Abrahamsen M, Salmeron J, Anic GM, Rollison DE, Smith D, 2011. Incidence and Clearance of Genital Human Papillomavirus Infection in Men (HIM): a Cohort Study 377. Lancet, London, England, 932–940.

Guergnon J, Godet AN, Galioot A, Falanga PB, Colle JH, Cayla X, Garcia A, 2011. PP2A targeting by viral proteins: a widespread biological strategy from DNA/RNA tumor viruses to HIV-1. Biochim. Biophys. Acta 1812, 1498–1507. [PubMed: 21856415]

Hampras SS, Giuliano AR, Lin HY, Fisher KJ, Abrahamsen ME, McKay-Chopin S, Gheit T, Tommasino M, Rollison DE, 2015. Natural history of polyomaviruses in men: the HPV infection in men (HIM) study. J. Infect. Dis 211, 1437–1446. [PubMed: 25387582]

Hampras SS, Giuliano AR, Lin HY, Fisher KJ, Abrahamsen ME, Sirak BA, Iannacone MR, Gheit T, Tommasino M, Rollison DE, 2014. Natural history of cutaneous human papillomavirus (HPV) infection in men: the HIM study. PLoS One 9, e104843. [PubMed: 25198694]

Ho J, Jedrych JJ, Feng H, Natalie AA, Grandinetti L, Mirvish E, Crespo MM, Yadav D, Fasanella KE, Proksell S, Kuan SF, Pastrana DV, Buck CB, Shuda Y, Moore PS, Chang Y, 2015. Human polyomavirus 7-associated pruritic rash and viremia in transplant recipients. J. Infect. Dis 211, 1560–1565. [PubMed: 25231015]

Houben R, Angermeyer S, Haferkamp S, Aue A, Goebeler M, Schrama D, Hesbacher S, 2015. Characterization of functional domains in the Merkel cell polyoma virus Large T antigen. Int. J. Cancer 136, E290–E300. [PubMed: 25208506]

Houben R, Adam C, Baeurle A, Hesbacher S, Grimm J, Angermeyer S, Henzel K, Hauser S, Elling R, Brocker EB, Gaubatz S, Becker JC, Schrama D, 2012. An intact retinoblastoma protein-binding site in Merkel cell polyomavirus large T antigen is required for promoting growth of Merkel cell carcinoma cells. Int. J. Cancer 130, 847–856. [PubMed: 21413015]

Jiang M, Abend JR, Johnson SF, Imperiale MJ, 2009. The role of polyomaviruses in human disease. Virology 384, 266–273. [PubMed: 18995875]

Johne R, Wittig W, Fernandez-de-Luco D, Hofle U, Muller H, 2006. Characterization of two novel polyomaviruses of birds by using multiply primed rolling-circle amplification of their genomes. J. Virol 80, 3523–3531. [PubMed: 16537620]

Johne R, Muller H, Rector A, van Ranst M, Stevens H, 2009. Rolling-circle amplification of viral DNA genomes using phi29 polymerase. Trends Microbiol. 17, 205–211. [PubMed: 19375325]

Johne R, Buck CB, Allander T, Atwood WJ, Garcea RL, Imperiale MJ, Major EO, Ramqvist T, Norkin LC, 2011. Taxonomical developments in the family Polyomaviridae. Arch. Virol 156, 1627–1634. [PubMed: 21562881]

Kean JM, Rao S, Wang M, Garcea RL, 2009. Seroepidemiology of Human polyomaviruses. PLoS Pathog. 5, e1000363. [PubMed: 19325891]

Kearse M, Moir R, Wilson A, Stones-Havas S, Cheung M, Sturrock S, Buxton S, Cooper A, Markowitz S, Duran C, Thierer T, Ashton B, Meintjes P, Drummond A, 2012. Geneious Basic: an Integrated and Extendable Desktop Software Platform for the Organization and Analysis of Sequence Data 28. Bioinformatics, Oxford, England, 1647–1649.

Koralnik IJ, 2006. Progressive multifocal leukoencephalopathy revisited: has the disease outgrown its name? Ann. Neurol 60, 162–173. [PubMed: 16862584]

Korup S, Rietscher J, Calvignac-Spencer S, Trusch F, Hofmann J, Moens U, Sauer I, Voigt S, Schmuck R, Ehlers B, 2013. Identification of a novel human polyomavirus in organs of the gastrointestinal tract. PLoS One 8, e58021. [PubMed: 23516426]

Kosugi S, Hasebe M, Tomita M,Yanagawa H, 2009b. Systematic identification of cell cycle-dependent yeast nucleocytoplasmic shuttling proteins by prediction of composite motifs. In: Proceedings of the National Academy of Sciences of the United States of America, vol. 106, pp. 10171–10176. [PubMed: 19520826]

Kosugi S, Hasebe M, Matsumura N, Takashima H, Miyamoto-Sato E, Tomita M, Yanagawa H, 2009a. Six classes of nuclear localization signals specific to different binding grooves of importin alpha. J. Biol. Chem 284, 478–485. [PubMed: 19001369]

Kumar S, Stecher G, Tamura K, 2016. MEGA7: molecular evolutionary genetics analysis version 7.0 for bigger datasets. Mol. Biol. Evol 33, 1870–1874. [PubMed: 27004904]

Kwun HJ, Shuda M, Camacho CJ, Gamper AM, Thant M, Chang Y, Moore PS, 2015. Restricted protein phosphatase 2A targeting by Merkel cell polyomavirus small T antigen. J. Virol 89, 4191–4200. [PubMed: 25631078]

Le SQ, Gascuel O, 2008. An improved general amino acid replacement matrix. Mol. Biol. Evol 25, 1307–1320. [PubMed: 18367465]

Li K, Zhang C, Zhao R, Xue Y, Yang J, Peng J, Jin Q, 2015. The prevalence of STL polyomavirus in stool samples from Chinese children. J. Clin. Virol.: Off. Publ. Pan Am. Soc. Clin. Virol 66, 19–23.

Lim ES, Reyes A, Antonio M, Saha D, Ikumapayi UN, Adeyemi M, Stine OC, Skelton R, Brennan DC, Mkakosya RS, Manary MJ, Gordon JI, Wang D, 2013. Discovery of STL polyomavirus, a polyomavirus of ancestral recombinant origin that encodes a unique T antigen by alternative splicing. Virology 436, 295–303. [PubMed: 23276405]

Miller NR, McKeever PE, London W, Padgett BL, Walker DL, Wallen WC, 1984. Brain tumors of owl monkeys inoculated with JC virus contain the JC virus genome. J. Virol 49, 848–856. [PubMed: 6321769]

Mishra N, Pereira M, Rhodes RH, An P, Pipas JM, Jain K, Kapoor A, Briese T, Faust PL, Lipkin WI, 2014. Identification of a novel polyomavirus in a pancreatic transplant recipient with retinal blindness and vasculitic myopathy. J. Infect. Dis 210, 1595–1599. [PubMed: 24795478]

Moens U, Johannessen M, 2008. Human polyomaviruses and cancer: expanding repertoire. J. Dtsch. Dermatol. Ges.=J. Ger. Soc. Dermatol.: JDDG 6, 704–708.

Moens U, Van Ghelue M, Johannessen M, 2007. Oncogenic potentials of the human polyomavirus regulatory proteins. Cell. Mol. Life Sci. : CMLS 64, 1656–1678. [PubMed: 17483871]

Nickeleit V, Singh HK, 2015. Polyomaviruses and disease: is there more to know than viremia and viruria? Curr. Opin. Organ Transplant 20, 348–358. [PubMed: 25933251]

Nunes EM, Sudenga SL, Gheit T, Tommasino M, Baggio ML, Ferreira S, Galan L, Silva RC, Pierce Campbell CM, Lazcano-Ponce E, Giuliano AR, Villa LL, Sichero L, 2016. Diversity of beta-papillomavirus at anogenital and oral anatomic sites of men: the HIM Study. Virology 495, 33–41. [PubMed: 27161202]

Padgett BL, Walker DL, ZuRhein GM, Eckroade RJ, Dessel BH, 1971. Cultivation of Papova-like Virus from Human Brain with Progressive Multifocal Leucoencephalopathy 1. Lancet, London, England, 1257–1260.

Peretti A, FitzGerald PC, Bliskovsky V, Pastrana DV, Buck CB, 2015. Genome Sequence of a Fish-Associated Polyomavirus, Black Sea Bass (Centropristis striata) Polyomavirus 1. Genome Announc, 3.

Pierce Campbell CM, Messina JL, Stoler MH, Jukic DM, Tommasino M, Gheit T, Rollison DE, Sichero L, Sirak BA, Ingles DJ, Abrahamsen M, Lu B, Villa LL, Lazcano-Ponce E, Giuliano AR, 2013. Cutaneous human papillomavirus types detected on the surface of male external genital lesions: a case series within the HPV Infection in Men Study. J. Clin. Virol. : Off. Publ. Pan Am. Soc. Clin. Virol 58, 652–659.

Pierce Campbell CM, Gheit T, Tommasino M, Lin HY, Torres BN, Messina JL, Stoler MH, Rollison DE, Sirak BA, Abrahamsen M, Carvalho da Silva RJ, Sichero L, Villa LL, Lazcano-Ponce E, Giuliano AR, 2016. Cutaneous beta human papillomaviruses and the development of male external genital lesions: a case-control study nested within the HIM Study. Virology 497, 314–322. [PubMed: 27518539]

Pipas JM, 1992. Common and unique features of T antigens encoded by the polyomavirus group. J. Virol 66, 3979–3985. [PubMed: 1318392]

Rector A, Tachezy R, Van Ranst M, 2004. A sequence-independent strategy for detection and cloning of circular DNA virus genomes by using multiply primed rolling-circle amplification. J. Virol 78, 4993–4998. [PubMed: 15113879]

Rennspiess D, Pujari S, Keijzers M, Abdul-Hamid MA, Hochstenbag M, Dingemans AM, Kurz AK, Speel EJ, Haugg A, Pastrana DV, Buck CB, De Baets MH, Zur Hausen A, 2015. Detection of human polyomavirus 7 in human thymic epithelial tumors. J. Thorac. Oncol. : Off. Publ. Int. Assoc. Study Lung Cancer 10, 360–366.

Rockett RJ, Sloots TP, Bowes S, O'Neill N, Ye S, Robson J, Whiley DM, Lambert SB, Wang D, Nissen MD, Bialasiewicz S, 2013. Detection of novel polyomaviruses, TSPyV, HPyV6, HPyV7, HPyV9 and MWPyV in feces, urine, blood, respiratory swabs and cerebrospinal fluid. PLoS One 8, e62764. [PubMed: 23667518]

Sablina AA, Hahn WC, 2008. SV40 small T antigen and PP2A phosphatase in cell transformation. Cancer Metastasis Rev. 27, 137–146. [PubMed: 18214640]

Schmitt M, Bravo IG, Snijders PJ, Gissmann L, Pawlita M, Waterboer T, 2006. Bead-based multiplex genotyping of human papillomaviruses. J. Clin. Microbiol 44, 504–512. [PubMed: 16455905]

Schmitt M, Dondog B, Waterboer T, Pawlita M, Tommasino M, Gheit T, 2010. Abundance of multiple high-risk human papillomavirus (HPV) infections found in cervical cells analyzed by use of an ultrasensitive HPV genotyping assay. J. Clin. Microbiol 48, 143–149. [PubMed: 19864475]

Schowalter RM, Pastrana DV, Pumphrey KA, Moyer AL, Buck CB, 2010. Merkel cell polyomavirus and two previously unknown polyomaviruses are chronically shed from human skin. Cell host Microbe 7, 509–515. [PubMed: 20542254]

Schuurman R, Sol C, van der Noordaa J, 1990. The complete nucleotide sequence of bovine polyomavirus. J. Gen. Virol 71 (Pt 8), 1723–1735. [PubMed: 2167926]

Scuda N, Hofmann J, Calvignac-Spencer S, Ruprecht K, Liman P, Kuhn J, Hengel H, Ehlers B, 2011.A novel human polyomavirus closely related to the african green monkey-derived lymphotropic polyomavirus. J. Virol 85, 4586–4590. [PubMed: 21307194]

Shollar D, Del Valle L, Khalili K, Otte J, Gordon J, 2004. JCV T-antigen interacts with the neurofibromatosis type 2 gene product in a transgenic mouse model of malignant peripheral nerve sheath tumors. Oncogene 23, 5459–5467. [PubMed: 15133494]

Shuda M, Feng H, Kwun HJ, Rosen ST, Gjoerup O, Moore PS, Chang Y, 2008. T antigen mutations are a human tumor-specific signature for Merkel cell polyomavirus. In: Proceedings of the National Academy of Sciences of the United States of America, vol. 105, pp. 16272–16277. [PubMed: 18812503]

Shuda M, Guastafierro A, Geng X, Shuda Y, Ostrowski SM, Lukianov S, Jenkins FJ, Honda K, Maricich SM, Moore PS, Chang Y, 2015. Merkel cell Polyomavirus small T antigen induces cancer and embryonic Merkel cell proliferation in a transgenic mouse model. PLoS One 10, e0142329. [PubMed: 26544690]

Shuda M, Arora R, Kwun HJ, Feng H, Sarid R, Fernandez-Figueras MT, Tolstov Y, Gjoerup O, Mansukhani MM, Swerdlow SH, Chaudhary PM, Kirkwood JM, Nalesnik MA, Kant JA, Weiss LM, Moore PS, Chang Y, 2009. Human Merkel cell polyomavirus infection I. MCV T antigen expression in Merkel cell carcinoma, lymphoid tissues and lymphoid tumors. Int. J. Cancer 125, 1243–1249. [PubMed: 19499546]

Siebrasse EA, Reyes A, Lim ES, Zhao G, Mkakosya RS, Manary MJ, Gordon JI, Wang D, 2012. Identification of MW polyomavirus, a novel polyomavirus in human stool. J. Virol 86, 10321–10326. [PubMed: 22740408]

Simmons DT, Loeber G, Tegtmeyer P, 1990. Four major sequence elements of simian virus 40 large T antigen coordinate its specific and nonspecific DNA binding. J. Virol 64, 1973–1983. [PubMed: 2157865]

Sroller V, Hamsikova E, Ludvikova V, Musil J, Nemeckova S, Salakova M, 2016. Seroprevalence rates of HPyV6, HPyV7, TSPyV, HPyV9, MWPyV and KIPyV polyomaviruses among the healthy blood donors. J. Med. Virol 88, 1254–1261. [PubMed: 26630080]

Toptan T, Yousem SA, Ho J, Matsushima Y, Stabile LP, Fernandez-Figueras MT, Bhargava R, Ryo A, Moore PS, Chang Y, 2016. Survey for human polyomaviruses in cancer. JCI Insight, 1.

van der Meijden E, Kazem S, Dargel CA, van Vuren N, Hensbergen PJ, Feltkamp MC, 2015. Characterization of T antigens, including middle T and alternative T, expressed by the human polyomavirus associated with trichodysplasia spinulosa. J. Virol 89, 9427–9439. [PubMed: 26136575]

van der Meijden E, Janssens RW, Lauber C, Bouwes Bavinck JN, Gorbalenya AE, Feltkamp MC, 2010. Discovery of a new human polyomavirus associated with trichodysplasia spinulosa in an immunocompromized patient. PLoS Pathog. 6, e1001024. [PubMed: 20686659]

Varakis J, ZuRhein GM, Padgett BL, Walker DL, 1978. Induction of peripheral neuroblastomas in Syrian hamsters after injection as neonates with JC virus, a human polyoma virus. Cancer Res. 38, 1718–1722. [PubMed: 206356]

Verhaegen ME, Mangelberger D, Harms PW, Vozheiko TD, Weick JW, Wilbert DM, Saunders TL, Ermilov AN, Bichakjian CK, Johnson TM, Imperiale MJ, Dlugosz AA, 2015. Merkel cell

polyomavirus small T antigen is oncogenic in transgenic mice. J. Investig. Dermatol 135, 1415–1424. [PubMed: 25313532]

Walker DL, Padgett BL, ZuRhein GM, Albert AE, Marsh RF, 1973. Human Papovavirus (JC): Induction of Brain Tumors in Hamsters 181. Science, New York, N.Y, 674–676.

Yu J, Boyapati A, Rundell K, 2001. Critical role for SV40 small-t antigen in human cell transformation. Virology 290, 192–198. [PubMed: 11883184]

Zu Rhein GM, Varakis JN, 1979. Perinatal induction of medulloblastomas in Syrian golden hamsters by a human polyoma virus (JC). Natl. Cancer Inst. Monogr, 205–208. [PubMed: 225669]

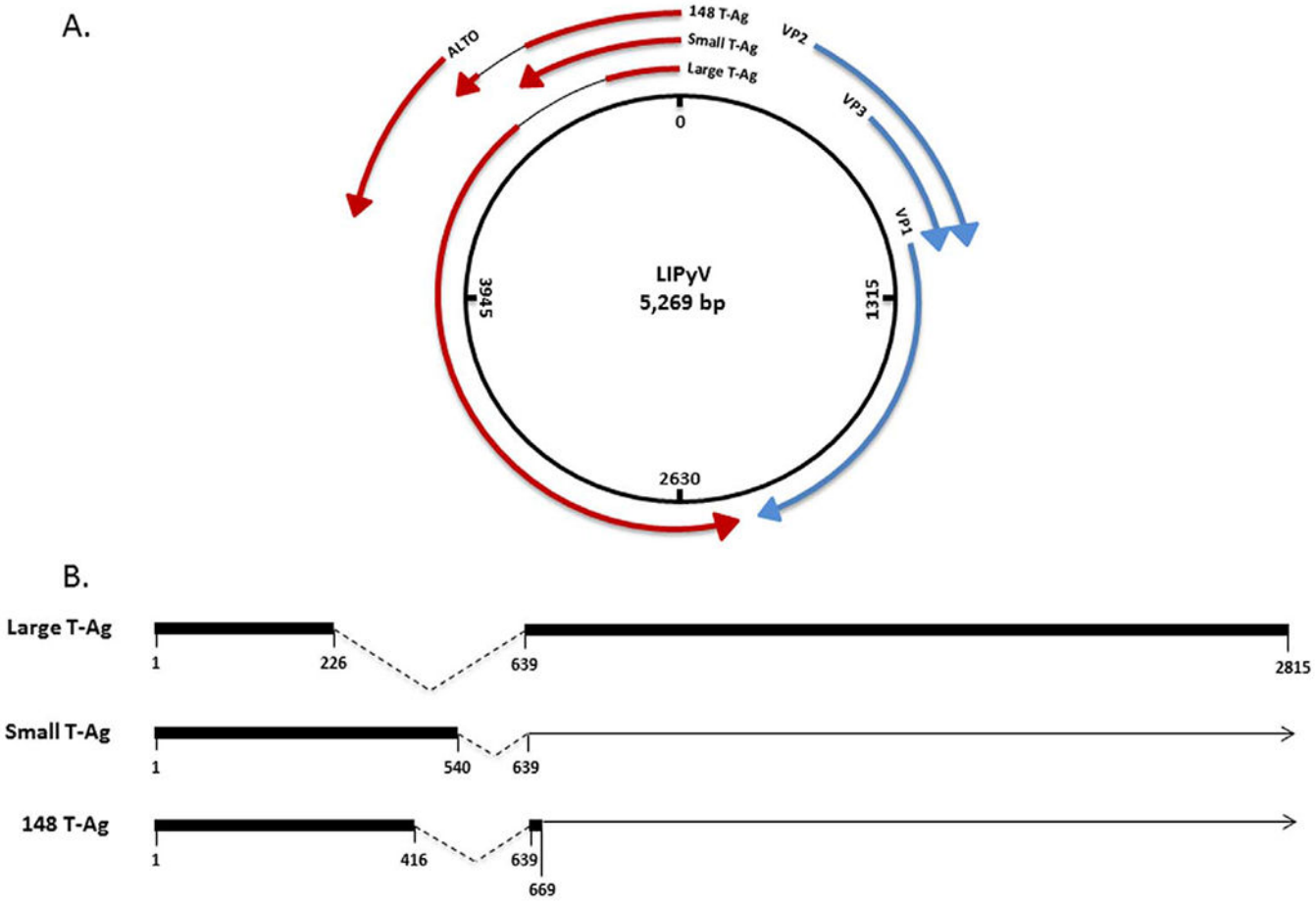

Fig. 1.

Genome organization of LIPyV. (A) The viral genome of 5269 bp comprises early and late coding regions that encode for two regulatory proteins (small T-antigen and large T-antigen), the 148 T-antigen, the putative alternate T antigen (ALTO), the major capsid protein VP1, and two minor capsid proteins, VP2 and VP3. These regions are separated by a non-coding control region (NCCR) of 401 bp. (B) Transcript mapping of small, large, and 148 T-antigens.

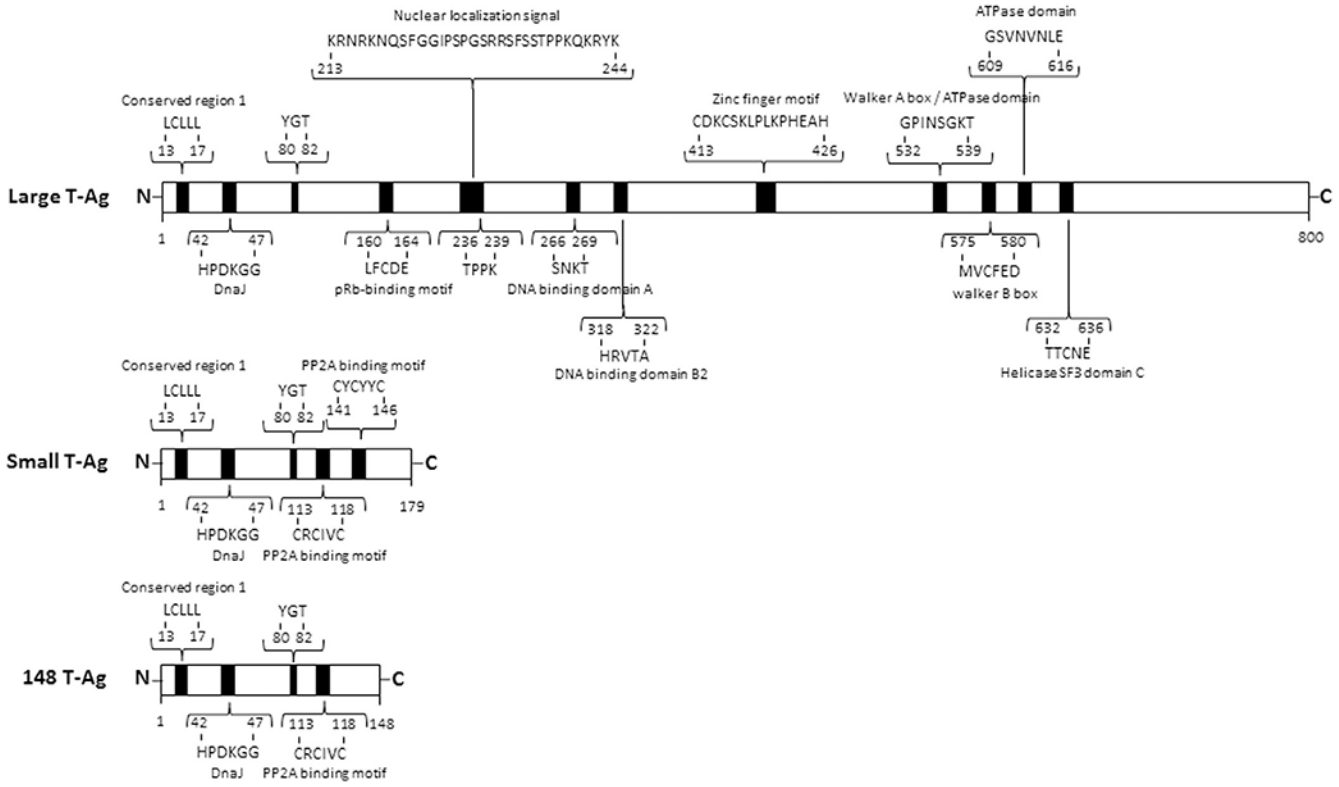

Fig. 2.

Structure of the large, small, and 148 T-antigens.

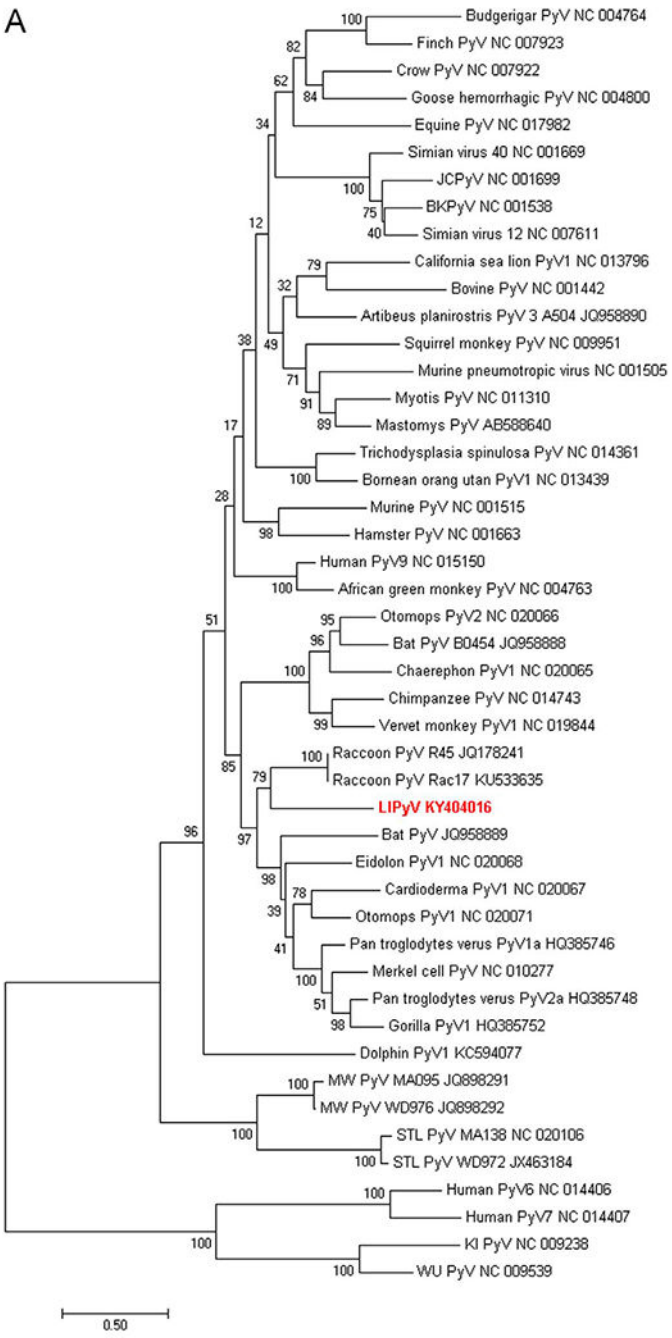

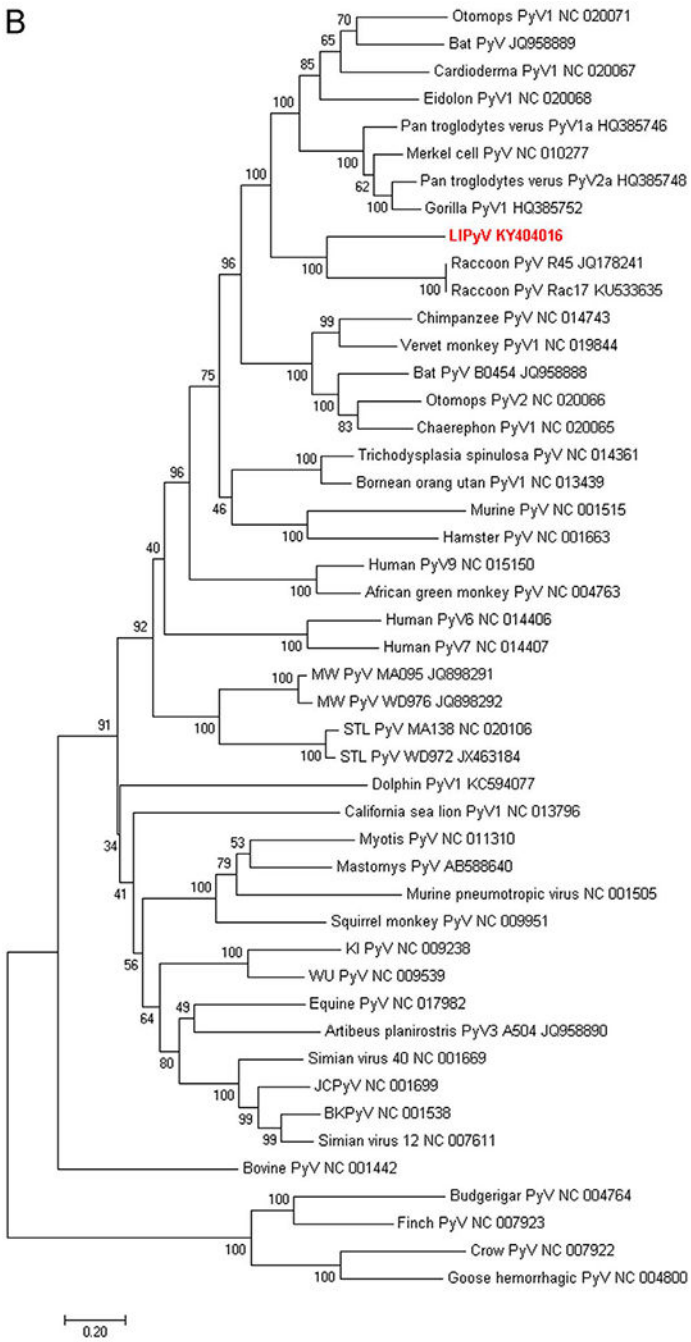

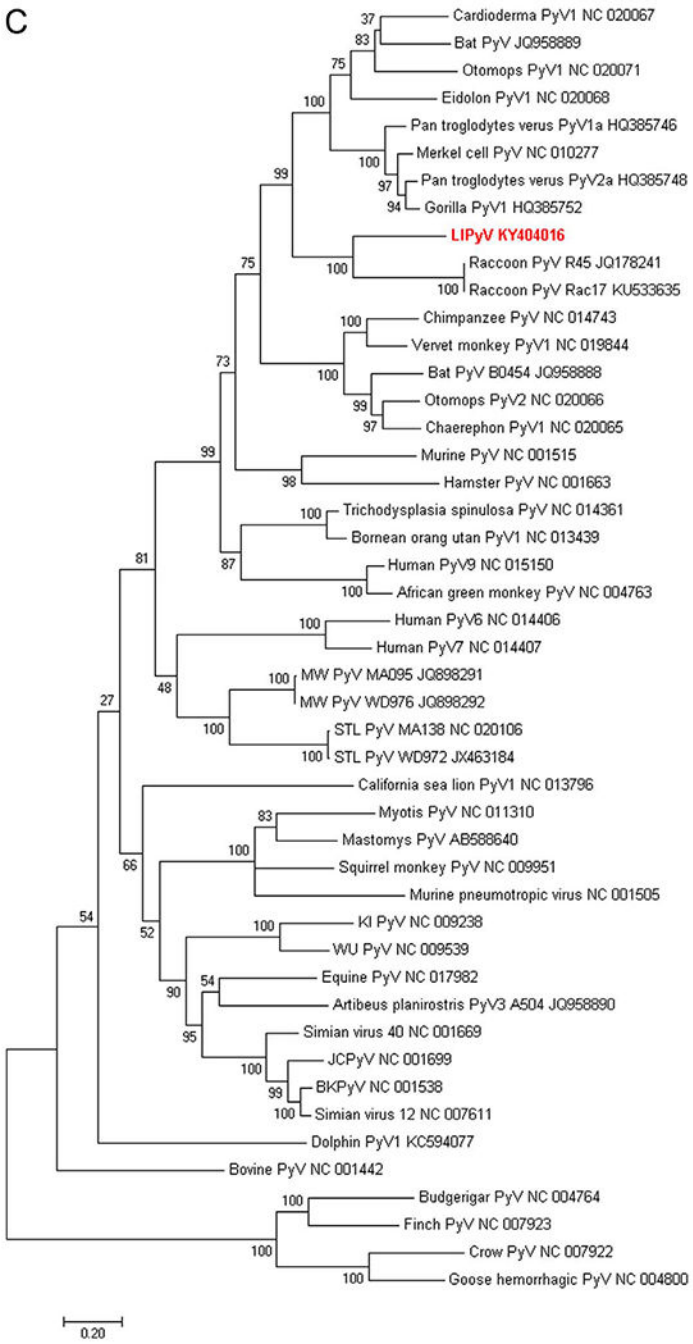

Fig. 3.

Maximum-likelihood phylogenetic unrooted trees produced from different regions of the LIPyV genome. The VP1 open reading frame (A), the large T-antigen (LT-Ag) open reading frame (B), and the amino acid sequence of LT-Ag (C) are compared separately. Scale bar shows substitution rate per site.

Virology. Author manuscript; available in PMC 2022 July 08.

Table 1

Description of the LIPyV T-antigens.

T-antigens	Amino acid motifs	Names	Amino acid positions	References
Large T-antigen				
	LCLLL	CR1	13–17	Pipas (1992)
	HPDKGG	DnaJ	42–47	
	YGT	YGT	80–82	Houben et al. (2015)
	LFCDE	pRB-binding motif	160–164	DeCaprio et al. (1988)
	KRNRKNQSFGGIPSPGSRRSFSSTPPKQKRYK	Nuclear localization signal *	213–244	Kosugi et al. (2009a) Kosugi et al. (2009b)
	TPPK	threonine–proline–proline–lysine	236–239	DeCaprio and Garcea (2013)
	SNKT	DNA-binding domain A	266–269	Johne et al. (2006)
	HRVTA	DNA-binding domain B2	318–322	Schuurman et al. (1990) Simmons et al. (1990)
	CDKCSKLPLKPHEAH	Zinc-finger motif	413–427	Ehlers and Moens (2014)
	GPINSGKT	Walker A box/ATPase domain	532–539	Pipas (1992)
	GSVNVNLE	ATPase domain	609–616	
	MVCFED	Walker B box	575–580	van der Meijden et al. (2010)
	TTCNE	Helicase superfamily 3 motif C	632–636	
Small T-antigen				
	LCLL	CR1	13–17	Pipas (1992)
	HPDKGG	DnaJ	42–47	
	YGT	YGT	80–82	Houben et al. (2015)
	CRCIVC	PP2A binding site	113–118	Pipas (1992)
	CYCYYC	PP2A binding site	141–146	
148 T-antigen				
	LCLL	CR1	13–17	Pipas (1992)
	HPDKGG	DnaJ	42–47	
	YGT	YGT	80–82	Houben et al. (2015)
	CRCIVC	PP2A binding site	113–118	Pipas (1992)

* A putative nuclear localization signal (NLS) has been predicted using an NLS-prediction algorithm, cNLS Mapper (http://nls-mapper.iab.keio.ac.jp/cgi-bin/NLS_Mapper_form.cgi).